Journal of Low Temperature Physics manuscript No.
(will be inserted by the editor)

Detector Calibration for the Micro-X Sounding Rocket X-ray Telescope

D.C. Goldfinger · J.S. Adams · R. Baker · S.R. Bandler · N. Bastidon · M.E. Danowski · W.B. Doriese · M.E. Eckart · E. Figueroa-Feliciano · S.N.T. Heine · G.C. Hilton · A.J.F. Hubbard · R.L. Kelley · C.A. Kilbourne · R.E. Manzagol-Harwood · D. McCammon · T. Okajima · F.S. Porter · C.D. Reintsema · P. Serlemitsos · S.J. Smith · P.Wikus

the date of receipt and acceptance should be inserted later

Abstract Micro-X is a sounding rocket borne X-ray telescope that uses a transition edge sensor microcalorimeter array to provide high energy resolution spectroscopy. Micro-X is a versatile instrument with plans to observe the Puppis A supernova remnant during its first flight, as well as future observations of the Milky Way to search for X-ray signals from decaying dark matter. Commissioning and functionality testing are complete and the thermal performance of the system has been validated. We are currently evaluating the detector performance in the flight cryostat with the flight multiplexing electronics. Operating in this setup has allowed us to characterize sources of detector and readout noise, as well as to implement mitigation techniques to improve performance in anticipation of the upcoming flight. We present an overview of important noise considerations in addition to an update on latest detector performance.

Keywords Sounding Rocket, Transition Edge Sensors, X-ray, Microcalorimeter

1 Introduction

Micro-X is an instrument that will use transition edge sensors (TESs) to perform high resolution microcalorimetry on astrophysical X-rays from a sounding rocket platform [1, 2]. The Micro-X array consists of 128 pixels arranged in a quasi-circular arrangement, to provide an 11.8 arcminute field-of-view. The absorbers are composed of 3.4 μm of bismuth with a 0.6 μm layer of gold, 590 μm per side, and the TESs are molybdenum/gold bilayers with a transition temperature of 120 mK [3]. Combined with the response of the X-ray mirror and the infrared blocking filters along the beam path, the bandpass of the instrument is between 0.1 and 2.5 keV [1]. The detector readout is achieved with a NIST SQUID time division multiplexing circuit with 8 columns consisting of 16 rows each [4]. The readout is split into two fully independent science chains with 4 columns each so any failures during flight will still leave half of the array operational.

Department of Physics, Massachusetts Institute of Technology,
Cambridge, MA 02139, United Sates of America
E-mail: dgoldfin@mit.edu

The 75 mK operating temperature of the detectors is achieved with an adiabatic demagnetization refrigerator, with a hold time at 75 mK of 9 hours [5]. This cryostat has passed vibration testing and is well suited for carrying the detectors on the sounding rocket platform [6]. That rocket provides an apogee of 270 km with 300 s above 160 km for the observation.

The first flight of Micro-X will observe the Bright Eastern Knot of the Puppis A supernova remnant. The combination of high energy resolution from microcalorimeter detectors and an imaging mirror will allow us to provide a significant improvement on the measured spectra in the soft X-ray band. For extended sources there are limits to the energy resolution achievable with grating spectrometers that do not apply to microcalorimeters because the spatial extent of the target blurs out the spectral information in gratings instruments whereas microcalorimeters measure the energy independently of any spatial information. As a bright target it is suitable for observation with a single sounding rocket flight, which makes it an ideal target for observation with Micro-X. The Micro-X spectrum will allow us to characterize the ionization states inside the target region, which will provide a definitive measurement to verify if charge exchange is occurring in this knot and will test the proposal of this region as a site for particle acceleration that results in cosmic rays. An alternate target (based on launch window availability) is Cassiopiea A, which shares similar characteristics. Future flights will search for unidentified lines coming from the Milky Way halo, such as would be expected from decays of a dark matter particle [7, 8].

2 Detector Resolution

2.1 Current Performance

The inherent resolution of the Micro-X TESs is 4.5 eV, which was measured at the NASA Goddard Space Flight Center (GSFC) in a mature, ground based cryostat that did not contribute additional noise to the system (Fig 1 Left). After installing the detectors into the flight cryostat, we then began the process of improving the readout hardware which involved redesigning significant components of the flight electronics to lower the noise to functional levels [9]. After these improvements, the energy resolution was measured to be 10 eV (Fig 1 Right). An increase in noise greater than what was expected from the addition of multiplexed readout was observed, leading to the worsened resolution. The difference in energy resolution was driven by excess low-frequency noise seen when the TESs were biased in the transition. This hints at the noise being coupled to the TES bias since excess noise passing through the SQUID biases would be seen independent of the state of the detector. This noise could be from the flight electronics or from the susceptibility to environmental noise passing through the feedthroughs into the cryostat. The design of those subsystems were made with operating under the stresses of a rocket flight in mind, so that introduced new design elements that needed to be vetted through testing with the actual detectors.

The difference in energy resolution manifested in two ways. The first was that measuring the average detector noise and average pulse height to generate a projected energy resolution from the integrated noise equivalent power (NEP) gave a figure of 7 eV (Fig 2). Additionally, measuring the full width at half maximum (FWHM) of the pulse height from noise traces gave 7 eV resolution, which is consistent with that projection. However, collecting pulses from an emission line to measure the FWHM energy resolution gave a resolution of 10 eV, which shows an added degradation. One contribution to the worsened resolution were sudden shifts in the gain within long exposure measurements that were difficult to properly correct for. These gain shifts were due to sudden changes in the baseline value of the first

stage SQUID feedback, which were caused by relocking of the flux locked loop on a single SQUID. When the relocking behaves correctly, it should return to the initial baseline value but in some cases it would lock at a different value, moving one flux quantum in the SQUID away from the original lockpoint. This led to the baseline on all other detectors that are multiplexed over the same SQUID feedback line having a small change in their own lockpoint, which produced a small change in gain from the new position in the SQUID V/Φ curve. By tuning the unlocked value of the SQUID feedback to be very near to the lockpoint, the locking software is able to reliably choose the same lockpoint every time eliminating these jumps and improving the energy resolution. Another contribution to the worsened resolution appears from a 60 Hz tone, derived from the mains electricity powering the electronics in the laboratory. This produces a dependence of the measured pulse height on the phase of 60 Hz noise that is present in the baseline data when the pulse arrives. Improved filtering in the data processing to eliminate this dependence is expected to further improve the measured resolution closer to the NEP.

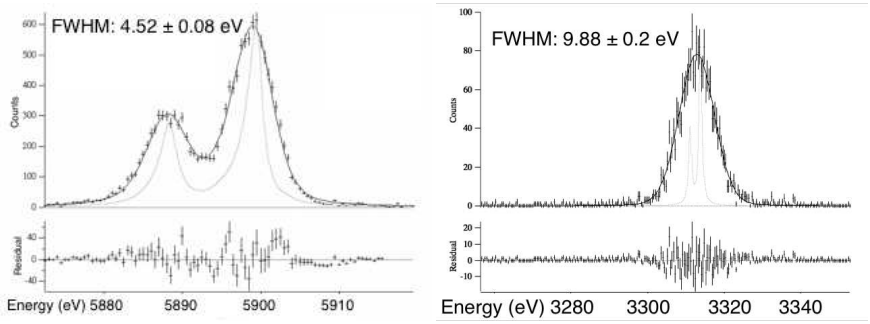

Fig. 1 Left: Measurement of the energy resolution of the Micro-X detectors in a laboratory cryostat at GSFC observing the Mn K-α line. Right: Measurement of the energy resolution in the flight cryostat after initial modifications to mitigate noise observing the K K-α line. (Color figure online.)

2.2 Noise Modeling

To understand the difference in performance between the detectors in the laboratory set-up and the flight set-up, we modeled the detectors using a preexisting package for modeling microcalorimeters in the IGOR programming language developed by members of the GSFC and Northwestern groups to try and generate the measured noise spectrum [10]. The inherent device parameters (conductance, heat capacity, squid coupling, steepness of transition, etc.) were measured in the flight system when possible and the design values were used for the other variables. By fitting the average pulse shape measured in the flight system to determine the bias point and steepness of the transition, the model projected a much lower noise spectrum than what we measured, where the modeled noise corresponded to the design resolution of 4.5 eV. By artificially increasing the amplitude of the phonon noise component but making no changes to the phonon noise shape, we were able to fit the measured noise spectrum over most frequencies, resulting in an NEP that matches the 7 eV measurement (Fig 2). This demonstrates that the component limiting the energy resolution generates a

phonon-like noise spectrum, which is a further hint that it couples into the TES directly through the bias current.

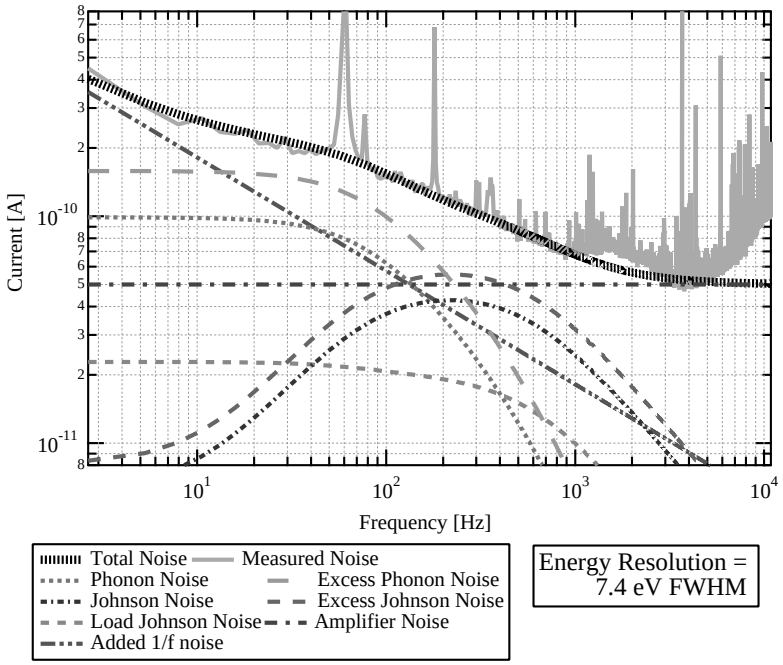

Fig. 2 Noise spectrum of a representative Micro-X pixel, prior to the modifications described in section 3. (Color figure online.)

Other differences between the modeled and measured noise spectra were the behavior at high frequencies and various lines at intermediate frequencies. There are a variety of sources for these lines, but are generally either generated by the control electronics or are pickup from the environment. With the exception of the 60 Hz noise, all of these lines are very sharp and have little impact on the achievable energy resolution and can be ignored. Even so, the sources of many of the lines were identified and eliminated so that the system would be as clean as possible [9]. The 60 Hz noise is not a problem in and of itself, since the rocket will have its own independent power in flight, instead of relying on electronics that are being powered by the 60 Hz AC mains electricity. However, the susceptibility to it suggests a possible explanation for other noise sources.

3 Noise Sources

3.1 Radio Frequency Pickup

In order to improve the performance of the Micro-X detectors, it is necessary to identify the source of the phonon-like noise. The extent of the noise varies from pixel to pixel, but does

not do so with any discernible pattern meaning that there is no correlation between pixels that share a detector bias and summing SQUID, nor between pixels that share a common lead for their first stage SQUID, nor for physical position within the array. Shot noise from an infrared light leak was proposed, but the performance of the detectors in the most recent run featuring an infrared filter on the detector box and the performance in the preceding run with a tightly sealed mylar sheet around the box opening showed minimal differences.

The leading explanation for the noise is pickup of radio frequency radiation from outside of the cryostat that is making its way into the cryostat. That the cryostat is susceptible to radiation was shown by operating an antenna radiating at 100 Hz in the vicinity of the cryostat. When the antenna was activated, the detector noise would increase and it would have a spectral response with the same shape as the phonon-like noise. The particular size of the response was inconsistent from day to day, but by observing the results on a live FFT generated by the readout software, we saw that the strength of the response would depend on which electrical connections were made to the feedthroughs where signals enter into the cryostat. Those connections are filtered, but the mechanical design does not eliminate all seams that might provide a path for radiation to enter into the interior. Applying metal foils over those openings as well as using metal tapes to provide conductance across those seams had minimal impact on the pickup from the antenna, however adding metal gaskets to the connectors did reduce the pickup. We expect that installing the gaskets on all connectors will lead to a reduction in the phonon-like noise during normal operation.

3.2 Downsampling of Digital Data

An additional component of the noise came about from the recording of digitized data in the readout electronics. After the data is digitized, it is downsampled by a factor of three so that the data rates for the entire system will be manageable for the flash memory being used. While the true sampling rate is well matched to the analog antialias filters on that circuit so that no aliased noise enters into the control loop for the SQUID flux locking, the effective sampling rate for the recorded data was lower which led to higher frequency noise being folded into lower part of the noise spectrum. By adding a finite impulse response digital filter into the firmware prior to downsampling, we were able to eliminate the high frequency information, uncovering the true noise response within the recorded bandwidth. This improved performance by eliminating the mischaracterized high frequency noise so that the signal to noise ratio was improved, but it also allows users to increase the proportional term in the PI feedback loop to allow it to quickly cancel out the error signals and maintain a more stable lock after a photon is absorbed, without producing an apparent increase in the noise at high frequencies. With this upgrade, as well as preliminary improvements to the shielding, we were able to measure a baseline resolution 4.6 eV (Fig 3).

4 Conclusion

The Micro-X detectors are currently performing at a level that will improve upon the energy resolution for imaging observations over existing X-ray observatories, but there is still room for improving the overall system's energy resolution. Installing the conductive gaskets into all connectors on the cryostat and external electronics will provide better shielding against pickup of radio frequency radiation, which should reduce the phonon-like noise which is the main driver of the baseline energy resolution. Other improvements, including the addition of

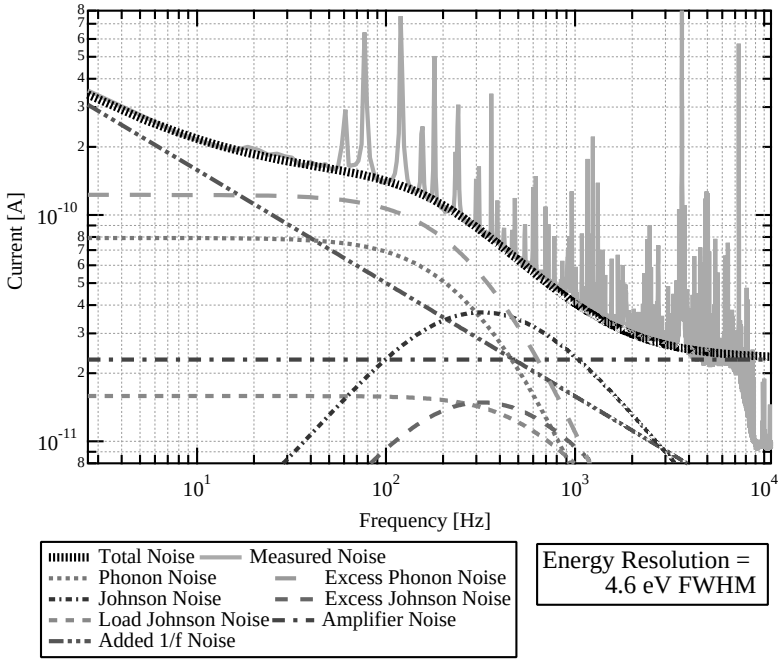

Fig. 3 Noise spectrum of a Micro-X pixel, after the addition of an antialias filter and improvements in the electrical shielding described in section 3. (Color figure online.)

digital antialias filtering prior to signal decimation and modifications to the tuning procedure to improve stability of the flux locked loop should lead to further improvements in the total detector performance. The energy resolution after these changes will be measured in an upcoming run, working towards the launch of the experiment in 2018.

Acknowledgements This work was supported by a NASA Space Technology Research Fellowship. The Micro-X project is conducted under NASA grant NNX10AE25G.

References

1. P. Wikus, J.S. Adams, R. Baker, S.R. Bandler, W. Brys, D. Dewey, W.B. Doriese, M.E. Eckart, E. Figueroa-Feliciano, R. Goeke, R. Hamersma, G.C. Hilton, U. Hwang, K.D. Irwin, R.L. Kelley, C.A. Kilbourne, S.W. Leman, D. McCammon, T. Okajima, R.H. O'Neal Jr., F.S. Porter, C.D. Reintsema, J.M. Rutherford, P. Serlemitsos, T. Saab, K. Sato, Y. Soong, and S.N. Trowbridge, *Proc. of the SPIE*, **7732**, 77321P, (2010), DOI:10.1117/12.857034
2. K.D. Irwin and G.C. Hilton, *Cryogenic Particle Detction*, ed. C. Enss, **99**, 63 (Springer, Berlin, 2005)
3. S.N.T. Heine, *PhD Dissertation, Massachusetts Institute of Technology* (2014)
4. W.B. Doriese, K.M. Morgan, D.A. Bennett, E.V. Denison, C.P. Fitzgerald, J.W. Fowler, J.D. Gard, J.P. Hays-Wehle, G.C. Hilton, K.D. Irwin, Y.I Joe, J.A.B. Mates, G.C. O'Neil, C.D. Reinstema, N.O. Robbins, D.R. Schmidt, D.S. Swetz, H. Tatsuno, L.R. Vale, and J.N. Ullom *J. Low Temp. Phys.*, **184**, 389, (2015), DOI:10.1007/s10909-015-1373-z
5. D.C. Goldfinger, E. Figueroa-Feliciano, M.E. Danowski, and S.N.T. Heine, *J. Low Temp. Phys.*, **184**, 699, (2016), DOI:10.1007/s10909-016-1549-1
6. M. E. Danowski, S. N. T. Heine, E. Figueroa-Feliciano, D. Goldfinger, P. Wikus, D. McCammon, and P. Oakley, *J. Low Temp. Phys.*, **184**, 597, (2016), DOI:10.1007/s10909-016-1580-2
7. E. Figueroa-Feliciano, A. Anderson, D. Castro, D.C Goldfinger, J. Rutherford, M. Eckart, R. Kelley, C. Kilbourne, D. McCammon, K. Morgan, F. Porter, and A. Szymkowiak, *ApJ*, **814**, 12, (2015), DOI:10.1088/0004-637X/814/1/82
8. A.J.F. Hubbard, J.S. Adams, R. Baker, S.R. Bandler, N. Bastidon, M.E. Danowski, W.B. Doriese, M.E. Eckart, E. Figueroa-Feliciano, D.C. Goldfinger, S.N.T. Heine, G.C. Hilton, R.L. Kelley, C.A. Kilbourne, R.E. Manzagol, D. McCammon, T. Okajima, F.S. Porter, C.D. Reintsema, P. Serlemitsos, S.J. Smith, and P. Wikus, *Proc. of 13th Rencontres du Vietnam*, submitted
9. D.C. Goldfinger, J.S. Adams, R. Baker, S.R. Bandler, M.E. Danowski, W.B. Doriese, M.E. Eckart, E. Figueroa-Feliciano, S.N.T. Heine, G.C. Hilton, A.J.F. Hubbard, R.L. Kelley, C.A. Kilbourne, D. McCammon, T. Okajima, F.S. Porter, C.D. Reintsema, P. Serlemitsos, S.J. Smith, and P. Wikus, *Proc. of the SPIE*, **9905**, 99054S, (2016), DOI:10.1117/12.2233299
10. Wavemetrics, *Igor Pro 7*, https://www.wavemetrics.com